HHS Public Access

Author manuscript

J Invest Dermatol. Author manuscript; available in PMC 2020 March 13.

Published in final edited form as:

J Invest Dermatol. 2017 November ; 137(11): 2336–2343. doi:10.1016/j.jid.2017.06.006.

Plasma PPi Deficiency is the Major, But Not the Exclusive, Cause of Ectopic Mineralization in an *Abcc6*$^{-/-}$ Mouse Model of PXE

Jingyi Zhao[1,2], **Joshua Kingman**[1], **John P. Sundberg**[3], **Jouni Uitto**[1,4], **Qiaoli Li**[1,4]

[1]Department of Dermatology and Cutaneous Biology, The Sidney Kimmel Medical College, and the PXE International Center of Excellence in Research and Clinical Care, Thomas Jefferson University, Philadelphia, PA 19107, USA

[2]Department of Dermatology, The First Affiliated Hospital of Zhejiang Chinese Medical University, Hangzhou 310006, China

[3]The Jackson Laboratory, Bar Harbor, Maine 04609, USA

[4]Jefferson Institute of Molecular Medicine, Thomas Jefferson University, Philadelphia, PA 19107, USA

Abstract

Pseudoxanthoma elasticum (PXE), a prototype of heritable ectopic mineralization disorders, is caused in most cases by inactivating mutations in the *ABCC6* gene. It was recently discovered that absence of ABCC6-mediated ATP release from the liver and consequently reduced plasma PPi levels underlie PXE. This study examined whether reduced levels of circulating PPi, an anti-mineralization factor, is the sole mechanism of PXE. The *Abcc6*$^{-/-}$ and *Enpp1*^{asj} mice were crossed with transgenic mice expressing human ENPP1, an ectonucleotidase which generates PPi from ATP. We generated *Abcc6*$^{-/-}$ and *Enpp1*^{asj} mice, either wild type or hemizygous for human *ENPP1*. Plasma levels of PPi and the degree of ectopic mineralization were determined. Overexpression of human ENPP1 in *Enpp1*^{asj} mice normalized plasma PPi levels to that of wild type mice, and consequently, completely prevented ectopic mineralization. These changes were accompanied with restoration of their bone microarchitecture. In contrast, while significantly reduced mineralization was noted in *Abcc6*$^{-/-}$ mice expressing human ENPP1, small mineralization foci were still evident despite increased plasma PPi levels. These results suggest that PPi is the major mediator of ectopic mineralization in PXE, but there might be an alternative, as-yet unknown mechanism, independent of PPi, by which ABCC6 prevents ectopic mineralization under physiologic conditions.

Keywords

Pseudoxanthoma elasticum; ectopic mineralization; mouse model; inorganic pyrophosphate

Address for Correspondence: Qiaoli Li, Ph.D., Department of Dermatology and Cutaneous Biology, The Sidney Kimmel Medical College at Thomas Jefferson University, 233 S. 10th Street, Suite 431 BLSB, Philadelphia, PA 19107, Qiaoli.Li@Jefferson.edu.

CONFLICTS OF INTEREST

JPS has a research contract with BIOCON LLC that has nothing to do with this project. All other authors declare no conflicts of interest.

INTRODUCTION

Ectopic mineralization, *i.e.*, deposition of calcium and phosphate complexes in soft connective tissues, is a global pathological problem. Ectopic mineralization has been encountered in several clinical conditions, including aging, cancer and diabetes as well as in autoimmune skin diseases (Giachelli, 1999). There are both acquired and heritable forms of ectopic mineralization in which the pathomechanistic pathways to connective tissue mineralization in different clinical conditions are poorly understood. Pseudoxanthoma elasticum (PXE), a multisystem disorder with variable phenotypic spectrum, is a prototype of a group of heritable ectopic mineralization disorders. Although ectopic mineralization affects a number of tissues in PXE, the clinical manifestations are primarily evident in the skin, eyes, and the cardiovascular system (Neldner, 1988). The initial cutaneous findings are usually yellowish papules that gradually coalesce to form lax and inelastic skin. The ophthalmologic findings consist of angioid streaks reflecting mineralization of Bruch's membrane behind the pigmented retina which allows growth of capillaries that eventually cover the retina, leading to loss of visual acuity and blindness. The cardiovascular complications include nephrogenic hypertension, intermittent claudication, and occasionally, early myocardial infarcts and stroke. PXE is characteristically a late-onset and slowly progressive disease with considerable intra- and interfamilial heterogeneity.

PXE is caused in most cases by mutations in the *ABCC6* gene (Bergen *et al.*, 2000; Le Saux *et al.*, 2000; Ringpfeil *et al.*, 2000). It encodes ATP-binding cassette subfamily C member 6 (ABCC6) which belongs to a family of ATP-binding cassette transmembrane transporters which are involved in the transport of a variety of substrates across cell membranes (Borst *et al.*, 2000; Dean *et al.*, 2001). Interestingly, ABCC6 is expressed primarily in the liver, to some extent in the kidneys, but at low levels, if at all, in tissues directly affected by mineralization in PXE (Belinsky and Kruh, 1999; Scheffer *et al.*, 2002). Several early observations, including reciprocal skin grafting and parabiosis experiments in *Abcc6*$^{-/-}$ mice and organ perfusion experiments in *Abcc6*$^{-/-}$ rats, support the current hypothesis that PXE is a metabolic disorder (Jiang *et al.*, 2009; Jiang *et al.*, 2010; Li *et al.*, 2017). This hypothesis postulates that deficient ABCC6 transport activity in the liver and kidneys results in lack of a circulating anti-mineralization factor(s) which under normal homeostatic conditions prevents ectopic mineralization in peripheral tissues (Li *et al.*, 2009; Uitto *et al.*, 2017).

It was recently demonstrated that ABCC6 mediates release of ATP from intracellular milieu to extracellular space, followed by rapid conversion of ATP to AMP and inorganic pyrophosphate (PPi) by ectonucleotide pyrophosphatase/phosphodiesterase 1 (ENPP1) (Jansen *et al.*, 2013; Jansen *et al.*, 2014). *ENPP1* mutations are associated with generalized arterial calcification of infancy (GACI), a heritable ectopic mineralization disorder with early onset and extensive vascular mineralization causing significant mortality in infancy due to essentially complete absence of plasma levels of PPi, a powerful inhibitor of mineralization (Rutsch *et al.*, 2003). It was recently shown that ABCC6-mediated ATP release is the main but not the sole source of circulating PPi. In support of this finding are recent observations that the plasma levels of PPi in the *Abcc6*$^{-/-}$ mice and in patients with PXE with complete absence of ABCC6 were low, ~30–40% of controls (Jansen *et al.*, 2013;

Jansen *et al.*, 2014). The finding of hepatic ABCC6-mediated ATP release was unexpected since ABCC6, similar to other members in the ABC transporter family, presumably utilizes the energy generated by intracellular ATP hydrolysis to maintain their transport activities. Nevertheless, ABCC6-mediated ATP release and subsequent conversion to plasma PPi by ENPP1 links the shared pathogenetic pathway from mutations in the *ABCC6* and *ENPP1* genes to plasma PPi deficiency and eventually ectopic mineralization (Uitto *et al.*, 2017).

Early development of *Abcc6*$^{-/-}$ mice provided model systems to examine the pathomechanisms and explore potential treatment modalities of PXE (Klement *et al.*, 2005). To investigate whether increasing plasma PPi levels in the *Abcc6*$^{-/-}$ mice would prevent ectopic mineralization, we crossed the *Abcc6*$^{-/-}$ mouse with a transgenic mouse with ubiquitous overexpression of human ENPP1 (Maddux *et al.*, 2006). As a control, the *Enpp1* mutant mice, *Enpp1*^{asj}, a model of GACI (Li *et al.*, 2013), were also crossed with human *ENPP1* transgenic mice. The results showed that overexpression of human ENPP1 increased plasma PPi levels in both *Abcc6*$^{-/-}$ and *Enpp1*^{asj} mice, and as a result, ectopic mineralization in the *Enpp1*^{asj} mice was completely absent. In contrast, small foci of ectopic mineralization were still present in the *Abcc6*$^{-/-}$ mice. These results suggest that lack of plasma PPi is not the sole mechanism by which ABCC6 prevents ectopic mineralization in PXE.

RESULTS

The *Abcc6*$^{-/-}$ mouse serves as a model to study PXE pathophysiology

In this study, we have utilized *Abcc6*$^{-/-}$ mice as a model system for PXE. As reported previously, these mice on standard rodent diet develop ectopic mineralization of connective tissues in a number of organs including skin, eyes, and arterial blood vessels (Klement *et al.*, 2005). A striking feature in these mice is mineralization of the connective tissue capsule surrounding the vibrissae in the muzzle skin which serves as an early reproducible biomarker of the mineralization process. The onset and extent of mineralization in the vibrissae and other tissues is, however, highly dependent on the mineral composition of the diet. Ectopic mineralization is enhanced in *Abcc6*$^{-/-}$ mice when they are placed on an “acceleration diet” enriched in phosphorus and low in magnesium (Jiang and Uitto, 2012; Li *et al.*, 2015). In addition, plasma PPi levels in the *Abcc6*$^{-/-}$ mice are reduced to ~30% of wild type mice (Jansen *et al.*, 2014).

The *Enpp1*^{asj} mouse serves as a model of GACI

The *Enpp1*^{asj} mutant mouse was derived from the ENU mutagenesis program at The Jackson Laboratory. These mice developed stiffening of the joints, hence the mutant mouse was named ‘ages with stiffened joints’ (*asj*). These mice harbor a missense mutation, p.V246D, in the *Enpp1* gene. We have shown that the mutant ENPP1 protein is largely absent in the *Enpp1*^{asj} mice, and the lack of enzymatic activity results in reduced PPi levels in the plasma (essentially zero), accompanied by extensive mineralization of a number of tissues. A greater extent of mineralization is observed in these mice when placed on acceleration diet. Thus, the *Enpp1*^{asj} mouse serves as a useful animal model for GACI (Li *et al.*, 2013).

The *Enpp1^{asj}* and *Abcc6$^{-/-}$* mice with overexpression of human *ENPP1* were generated by breeding the *Enpp1^{asj}* or *Abcc6$^{-/-}$* mouse with a human *ENPP1* transgenic mouse

If reduced plasma PPi levels underlie PXE, it is expected that increasing plasma levels of PPi would prevent ectopic mineralization in PXE caused by *ABCC6* mutations. To this end, we have taken advantage of a transgenic mouse with ubiquitous expression of human ENPP1 protein (Maddux *et al.*, 2006). Characterization of these mice by Western blots revealed human ENPP1 protein expression in a variety of tissues (Fig. S1).

The *Abcc6$^{-/-}$* mice were crossed with human *ENPP1* transgenic mice (*hENPP1$^{Tg/0}$*). As a positive control, the *Enpp1^{asj}* mice were also crossed with human *ENPP1* transgenic mice which compensate for the loss of the mouse endogenous ENPP1 protein. Thus, the *Abcc6$^{-/-}$;hENPP1$^{0/0}$*, *Enpp1^{asj};hENPP1$^{0/0}$* and the corresponding *Abcc6$^{-/-}$;hENPP1$^{Tg/0}$* and *Enpp1^{asj};hENPP1$^{Tg/0}$* mice were generated. These mice, including wild type (*WT*) and *hENPP1$^{Tg/0}$* mice, were placed on acceleration diet at 4 weeks of age (Table 1).

Overexpression of human ENPP1 completely prevents connective tissue mineralization in *Enpp1^{asj}* mice but not in *Abcc6$^{-/-}$* mice

At 12 weeks of age all the mice were euthanized. The degree of ectopic connective tissue mineralization was determined by two independent assays. The right side of muzzle skin containing vibrissae, right kidney, right pinna, eyes, heart, descending thoracic aorta, and spleen were processed for semi-quantitative histopathologic examinations. Calcium in tissues from the left side of muzzle skin, left kidney, left pinna, and abdominal aorta was solubilized and quantitated using a chemical assay.

Alizarin red stains revealed extensive mineralization in the *Enpp1^{asj};hENPP1$^{0/0}$* mice in a number of tissues (Fig. 1a, upper row). In contrast, the *Enpp1^{asj};hENPP1$^{Tg/0}$* mice had no evidence of mineralization (Fig. 1a, lower row; Table S1), suggesting that the human ENPP1 is a functional ortholog of mouse ENPP1. The calcium assay demonstrated that the amount of calcium in the tissues of muzzle skin, kidney, pinna, and abdominal aorta in *Enpp1^{asj};hENPP1$^{Tg/0}$* mice was similar to that of *WT* mice devoid of ectopic mineralization (Fig. 2a). In addition, mineralization was also absent in other tissues examined by histology (Table S1). The lack of ectopic mineralization also had physiologic consequences. The *Enpp1^{asj};hENPP1$^{0/0}$* mice showed stiffened joints with limited movement, while the *Enpp1^{asj};hENPP1$^{Tg/0}$* mice had a dramatic failure to develop joint abnormalities (Supplementary Movie 1).

As compared to *Abcc6$^{-/-}$;hENPP1$^{0/0}$* mice (Fig. 1b, upper row), the *Abcc6$^{-/-}$;hENPP1$^{Tg/0}$* mice showed significantly reduced mineralization in the muzzle skin and kidney; however, distinct mineralization foci were still evident (Fig. 1b, lower row). The calcium assay showed significant reduction in the amount of calcium in the muzzle skin (72%) and kidney (45%) in *Abcc6$^{-/-}$;hENPP1$^{Tg/0}$* mice, however, the calcium content was still significantly higher than those of *WT* mice (Fig. 2b). Residual mineralization was also present in other tissues (Table S1). Despite the use of acceleration diet, these tissues in *Abcc6$^{-/-}$* mice were not reproducibly mineralized, therefore, only histologic examination was performed in these tissues. No gender differences were observed in different groups of mice.

Plasma PPi levels were increased in *Enpp1^{asj};hENPP1$^{Tg/0}$* and *Abcc6$^{-/-}$;hENPP1$^{Tg/0}$* mice

To further examine the consequences of human ENPP1 overexpression, PPi levels were determined in plasma of *WT*, *hENPP1$^{Tg/0}$* transgenic mice, and *Abcc6$^{-/-}$* and *Enpp1^{asj}* mice with and without human ENPP1 overexpression (Table 2). The results demonstrated significantly increased plasma PPi levels in *hENPP1$^{Tg/0}$* mice as compared to *WT* mice. Consistent with previous results, the *Enpp1^{asj};hENPP1$^{0/0}$* mice had essentially no plasma PPi, indicating that PPi is generated by ENPP1 hydrolysis of ATP. In contrast, plasma PPi levels in the *Abcc6$^{-/-}$;hENPP1$^{0/0}$* mice were ~30% from the *WT* controls. Overexpression of human ENPP1 in either *Enpp1^{asj}* or *Abcc6$^{-/-}$* mice significantly increased plasma PPi levels to that of *WT* mice, with a concomitant increase in the PPi/Pi ratio (Table 2). The serum calcium and phosphorus levels and the corresponding Ca/Pi ratios were not statistically different between these groups of mice (Table 2). No gender differences were observed in different groups of mice.

Overexpression of human ENPP1 restores bone microarchitecture in *Enpp1^{asj}* mice

The femurs were dissected from *WT*, *Enpp1^{asj};hENPP1$^{0/0}$* and *Enpp1^{asj};hENPP1$^{Tg/0}$* mice for evaluation of their bone microarchitecture as a result of changes in plasma PPi levels. Consistent with previous results, significant hypomineralization of the femur was observed by microcomputed tomography in the *Enpp1^{asj}* mice as compared to sex-matched *WT* mice (Fig. 3). Sex-matched comparisons were performed due to sex difference in bone microarchitecture (Li *et al.*, 2016b). These changes of bone morphometric microarchitecture were subsequently quantified using a manufacturer-provided software (Table 3). Specifically, the trabecular bone of *Enpp1^{asj}* mice of both sexes have significantly decreased trabecular number and increased trabecular separation, corresponding to decreased trabecular bone mineral density and bone volume fraction. The structural model index was significantly higher and the connectivity density was significantly lower. The cortical bone mineral density and cortical thickness were significantly decreased, while the cortical porosity was increased (Table 3). The *Enpp1^{asj};hENPP1$^{Tg/0}$* mice had most of the trabecular and cortical bone parameters close to those in the *WT* mice indicating the protective effect of the transgene.

DISCUSSION

PPi has long been known as a by-product of many intracellular biosynthetic reactions, and was first identified as a key endogenous inhibitor of biomineralization in the 1960s (Fleisch and Bisaz, 1962c, b, a; Fleisch and Neuman, 1961). The direct effects of PPi on hydroxyapatite formation have been well established. PPi acts as a potent inhibitor of mineralization by binding strongly to the surface of nascent or growing hydroxyapatite crystals, thereby blocking their ability to act as a nidus for mineralization therefore preventing further crystal growth. This mechanism of action through direct inhibition of hydroxyapatite crystal formation thereby acts as a physiological ‘water-softener’ which will prevent harmful soft tissue mineralization and regulate bone mineralization (Orriss *et al.*, 2016). The concept and the importance of plasma PPi as a powerful anti-mineralization factor are emphasized by a number of clinical conditions in the spectrum of heritable ectopic mineralization disorders (Uitto *et al.*, 2017). Specifically, mutations in genes encoding PPi-

regulating proteins, such as ABCC6, ENPP1, ecto-5'-nucleotidase (CD73), and ANK, cause ectopic mineralization phenotypes (Orriss *et al.*, 2016).

ENPP1 mutations are associated with GACI which has overlapping phenotypic features with PXE; however, GACI is frequently a lethal disease in which fetus develop severe mineralization of the arteries and expire of cardiac failure as neonates. PXE and GACI can be caused by *ABCC6* and *ENPP1* mutations (Li *et al.*, 2012; Nitschke *et al.*, 2012). These observations suggested the possibility of shared pathomechanistic pathways for these conditions. The pathogenetic role of *ENPP1* mutations to ectopic mineralization in GACI has been made by demonstration that ENPP1 converts ATP to PPi which plays a crucial role as an inhibitor of mineralization. This coincides with the observation that ectopic mineralization in $Enpp1^{-/-}$ mice depends on plasma PPi levels and not local PPi production (Lomashvili *et al.*, 2014). ABCC6 is a putative ATP-dependent efflux transporter present mainly in the liver. It was recently reported that ABCC6 mediates ATP release from the liver and released ATP is converted by ENPP1 into PPi (Jansen *et al.*, 2014). The unanticipated role of ABCC6-dependent ATP release was supported by reduced plasma PPi concentrations in patients with PXE and in $Abcc6^{-/-}$ mice to be ~30–40% of those found in controls (Jansen *et al.*, 2014). Thus, deficiencies in ABCC6 and ENPP1 proteins lead to reduced plasma PPi levels and PPi/Pi ratio. These findings support the concept that the lack of hepatic ABCC6-dependent release of ATP is the critical pathogenic feature in PXE, and that PPi might be the circulating factor whose deficiency allows ectopic mineralization of the peripheral tissues, such as skin, eyes, and the arterial blood vessels, to take place (Jansen *et al.*, 2014).

The present study challenges the notion that the lack of ABCC6-dependent release of ATP in the liver and plasma PPi deficiency is the only pathomechanism of PXE. To test this hypothesis, we increased plasma PPi levels in the $Abcc6^{-/-}$ and $Enppl^{asj}$ mice by overexpression of ENPP1 by taking advantage of an available transgenic mouse expressing human *ENPP1* driven by a CMV promoter. Not surprisingly, plasma PPi levels in $Enpp1^{asj};hENPP1^{Tg/0}$ mice were restored to that of *WT* mice. As a result of substantial increase of plasma PPi levels, ectopic mineralization was entirely absent in the $Enpp1^{asj};hENPP1^{Tg/0}$ mice with concomitant improvements in bone microarchitecture, suggesting that *ENPP1* gene therapy could represent a promising approach for GACI for which there is currently no effective treatments. Recently, it was shown that recombinant ENPP1-Fc fusion enzyme, when administered subcutaneously in $Enpp1^{asj}$ mice prevents mortality and vascular mineralization (Albright *et al.*, 2015). Similar to $Enpp1^{asj};hENPP1^{Tg/0}$ mice, plasma PPi levels in $Abcc6^{-/-};hENPP1^{Tg/0}$ mice were increased from ~30–40% of *WT* controls in $Abcc6^{-/-}$ mice to that of *WT* controls; however, residual mineralization was still present in the $Abcc6^{-/-};hENPP1^{Tg/0}$ mice. The early seminal work reported that under physiologic conditions, ABCC6-mediated ATP release in the liver serves as the main source for formation of plasma PPi (Jansen *et al.*, 2014). These results suggest that while the majority, ~60–70%, of plasma PPi is derived from ATP in an ABCC6-dependent manner, a significant fraction, ~ 30–40%, originates from ATP released by ABCC6-independent means. The increased plasma PPi levels in the $Abcc6^{-/-};hENPP1^{Tg/0}$ mice probably reflect PPi generated by ENPP1 from other tissues independent of ABCC6.

Taken together, we show that the mechanism of ABCC6-mediated ATP release and subsequent conversion to PPi in plasma does not fully explain why absence of ABCC6 results in ectopic mineralization in PXE. The results suggest that plasma PPi deficiency is the major, albeit not the only, mechanism of connective tissue mineralization in PXE. There appears to be a second, as-yet unknown mechanism independent of PPi, by which ABCC6 prevents ectopic mineralization in PXE under physiologic conditions. Other mechanisms by which ABCC6 prevents ectopic mineralization have yet to be identified. Specifically, identification of the molecule(s) transported by ABCC6 is critical in understanding the pathophysiology of PXE. Nevertheless, overexpression of human ENPP1 augmented plasma PPi levels and significantly reduced the degree of ectopic mineralization in the *Abcc6*$^{-/-}$ mouse model of PXE. The results suggest that increasing plasma PPi to normal levels could inhibit or slow down progression even though does not completely prevent ectopic mineralization in PXE. Identification of additional mechanisms for ectopic mineralization in PXE may provide other therapeutic strategies. The significance obtained from this study may be applicable to many common diseases, such as chronic kidney disease, atherosclerosis, diabetes mellitus, and autoimmune inflammatory skin diseases (scleroderma, dermatomyositis, and systemic lupus erythematosus), which are accompanied by ectopic mineralization. Mechanisms shown to prevent ectopic mineralization in PXE are likely also to ameliorate ectopic mineralization seen in these disorders with significant morbidity and mortality in general population, although the specific pathomechanistic pathways of ectopic mineralization need to be determined to support this hypothesis.

MATERIALS AND METHODS

Mice, diets and breeding

The *Abcc6*^{tm1JfK} mouse model of PXE (referred to in this study as *Abcc6*$^{-/-}$ mice) was developed by targeted ablation of the *Abcc6* gene, as described previously (Klement *et al.*, 2005). Heterozygous alleles were backcrossed for ten generations into the C57BL/6J background. C57BL/6J-*Enpp1*^{asj}/GrsrJ mice were obtained from The Jackson Laboratory (Bar Harbor, ME). These homozygous mutant mice are referred to in this publication as the *Enpp1*^{asj} mice (Li *et al.*, 2013). The transgenic mice with ubiquitous overexpression of human ENPP1 were obtained from the Mutant Mouse Regional Resource Center at University of California Davis by cryo-recovery (B6;FVB-Tg(CMV-NPP1)1Brem/Mmucd). These mice were crossed with C57BL/6J mice to generate transgenic mice (*hENPP1*$^{Tg/0}$) on an incipient congenic C57BL/6J background. Compound *Abcc6;hENPP1* and *Enpp1;hENPP1* transgenic mice were generated by intercrossing *hENPP1*$^{Tg/0}$ mice with *Abcc6*$^{-/-}$ mice and *Enpp1*^{asj} mice, respectively.

The mice were maintained on a standard rodent diet (Laboratory Rodent Diet 5010; PMI Nutrition, Brentwood, MO, USA) in the Animal Facility of the Thomas Jefferson University. The pups at 4 weeks of age were placed on an acceleration diet with specific mineral modifications (Harlan Teklad, Rodent diet TD.00442, Madison, WI, USA). The acceleration diet is enriched in phosphorus (2X) and has reduced magnesium content (20%) in comparison to the standard control rodent diet. The animal studies were approved by the Institutional Animal Care and Use Committee of Thomas Jefferson University.

Western blot

Tissue lysates were prepared by homogenizing tissues in lysis buffer containing PMSF (Sigma, St Louis, MO), phosphatase inhibitor cocktail (Sigma), protease inhibitor cocktail (Thermo Scientific, Rockford, IL) and 8 M urea (Fisher, Pittsburgh, PA) in RIPA buffer (Sigma). A BCA kit (Thermo Scientific) was used to determine the protein concentration of all lysates. The primary antibodies were rabbit anti-ENPP1 antibody (Cell Signaling, Danvers, MA) and mouse anti-β-actin antibody (Abcam, Cambridge, MA), respectively. The secondary antibodies were anti-rabbit and anti-mouse antibody (LI-COR, Lincoln, NE). Images were acquired from an Odyssey Infrared Imager (LI-COR).

Histopathological analysis

Muzzle skin biopsies (right side), right kidney, descending thoracic aorta, right pinna, eyes, heart, and spleen from euthanized mice were collected and processed for histology. Tissue sections were stained with hematoxylin and eosin or Alizarin red using standard procedures.

Chemical quantitation of calcium and phosphate

To quantify the calcium deposition in mouse tissues, the left muzzle skin (which contains the vibrissae), left kidney, abdominal aorta, and left pinna, were harvested and solubilized with 1 N HCl for 48 h at room temperature. The solubilized calcium content in these tissues was determined colorimetrically by the Ó-cresolphthalein complexone method (Calcium (CPC) Liquicolor; Stanbio Laboratory, Boerne, TX, USA). The values for calcium in different tissues were normalized to tissue weight. Calcium in the plasma samples were determined with the same assay. The plasma phosphate content was measured by the Malachite Green Phosphate Assay kit (BioAssay Systems, Hayward, CA, USA).

Plasma collection and inorganic pyrophosphate (PPi) assay

Whole blood was collected by cardiac puncture into heparin containing syringe, transferred into a test tube and stored on ice. After centrifugation, plasma was depleted of platelets by filtration through a Centrisart I 300 kD mass cutoff filter (Sartorius, New York, NY, USA) and stored at −80°C until further processing (Tolouian *et al.*, 2012). PPi in plasma was measured by an enzymatic reaction using ATP sulfurylase to convert PPi into ATP in the presence of excess adenosine 5’ phosphosulfate (Sigma-Aldrich, St. Louis, MO, USA), as described previously (Jansen *et al.*, 2014; Li *et al.*, 2017).

Microcomputed tomography

The microarchitecture of the distal trabecular bone and mid-shaft region of the right femur was analyzed as described previously using the microcomputed tomography system (μCT35; Scanco Medical AG, Bassersdorf, Switzerland) (Li *et al.*, 2016).

Statistical analysis

The results in different groups of mice receiving various diets were first analyzed for normal distribution using Hamilton’s test. Comparisons of continuous measures across all groups were completed using two-sided Kruskal–Wallis nonparametric tests. Fisher’s exact test was

used to determine the difference between proportions of mineralization in different tissues of mice.

Supplementary Material

Refer to Web version on PubMed Central for supplementary material.

ACKNOWLEDGEMENTS

The authors thank Dian Wang for technical assistance. The authors acknowledge Penn Center for Musculoskeletal Disorders, supported by NIH/NIAMS P30AR050950, and Dr. Michael Levine, for assistance in the analysis of bone morphometry. Carol Kelly assisted in manuscript preparation. Dr. Li is recipient of a NIH Career Development Award (K01AR064766). This study was supported by NIH grant R01AR55225 (JU).

Abbreviations:

PXE	pseudoxanthoma elasticum
GACI	generalized arterial calcification of infancy
WT	wild type
asj	ages with stiffened joints
Pi	inorganic phosphate
PPi	inorganic pyrophosphate

REFERENCES

Albright RA, Stabach P, Cao W, Kavanagh D, Mullen I, Braddock AA, et al. ENPP1-Fc prevents mortality and vascular calcifications in rodent model of generalized arterial calcification of infancy. Nat Commun 2015;6:10006. [PubMed: 26624227]

Belinsky MG, Kruh GD. MOAT-E (ARA) is a full-length MRP/cMOAT subfamily transporter expressed in kidney and liver. Br J Cancer 1999;80:1342–9. [PubMed: 10424734]

Bergen AA, Plomp AS, Schuurman EJ, Terry S, Breuning M, Dauwerse H, et al. Mutations in ABCC6 cause pseudoxanthoma elasticum. Nat Genet 2000;25:228–31. [PubMed: 10835643]

Borst P, Evers R, Kool M, Wijnholds J. A family of drug transporters: the multidrug resistance-associated proteins. J Natl Cancer Inst 2000;92:1295–302. [PubMed: 10944550]

Dean M, Hamon Y, Chimini G. The human ATP-binding cassette (ABC) transporter superfamily. J Lipid Res 2001;42:1007–17. [PubMed: 11441126]

Fleisch H, Neuman W. The role of phosphatase and polyphosphates in calcification of collagen. Helv Physiol Pharmacol Acta 1961;19:C17–8. [PubMed: 13700175]

Fleisch H, Bisaz S. The inhibitory role of pyrophosphate in calcification. J Physiol (Paris) 1962a;54:340–1. [PubMed: 13893488]

Fleisch H, Bisaz S. Mechanism of calcification: inhibitory role of pyrophosphate. Nature 1962b;195:911.

Fleisch H, Bisaz S. Isolation from urine of pyrophosphate, a calcification inhibitor. Am J Physiol 1962c;203:671–5. [PubMed: 13945462]

Giachelli CM. Ectopic calcification: gathering hard facts about soft tissue mineralization. Am J Pathol 1999;154:671–5. [PubMed: 10079244]

Jansen RS, Kucukosmanoglu A, de Haas M, Sapthu S, Otero JA, Hegman IE, et al. ABCC6 prevents ectopic mineralization seen in pseudoxanthoma elasticum by inducing cellular nucleotide release. Proc Nat Acad Sci USA 2013;110:20206–11. [PubMed: 24277820]

Jansen RS, Duijst S, Mahakena S, Sommer D, Szeri F, Varadi A, et al. ABCC6-mediated ATP secretion by the liver is the main source of the mineralization inhibitor inorganic pyrophosphate in the systemic circulation-brief report. Arterioscler Thromb Vasc Biol 2014;34:1985–9. [PubMed: 24969777]

Jiang Q, Endo M, Dibra F, Wang K, Uitto J. Pseudoxanthoma elasticum is a metabolic disease. J Invest Dermatol 2009;129:348–54. [PubMed: 18685618]

Jiang Q, Oldenburg R, Otsuru S, Grand-Pierre AE, Horwitz EM, Uitto J. Parabiotic heterogenetic pairing of Abcc6−/−/Rag1−/− mice and their wild-type counterparts halts ectopic mineralization in a murine model of pseudoxanthoma elasticum. Am J Pathol 2010;176:1855–62. [PubMed: 20185580]

Jiang Q, Uitto J. Restricting dietary magnesium accelerates ectopic connective tissue mineralization in a mouse model of pseudoxanthoma elasticum (Abcc6−/−). Exp Dermatol 2012;21:694–9. [PubMed: 22897576]

Klement JF, Matsuzaki Y, Jiang QJ, Terlizzi J, Choi HY, Fujimoto N, et al. Targeted ablation of the Abcc6 gene results in ectopic mineralization of connective tissues. Mol Cell Biol 2005;25:8299–310. [PubMed: 16135817]

Le Saux O, Urban Z, Tschuch C, Csiszar K, Bacchelli B, Quaglino D, et al. Mutations in a gene encoding an ABC transporter cause pseudoxanthoma elasticum. Nat Genet 2000;25:223–7. [PubMed: 10835642]

Li Q, Jiang Q, Pfendner E, Varadi A, Uitto J. Pseudoxanthoma elasticum: clinical phenotypes, molecular genetics and putative pathomechanisms. Exp Dermatol 2009;18:1–11. [PubMed: 19054062]

Li Q, Schumacher W, Siegel D, Jablonski D, Uitto J. Cutaneous features of pseudoxanthoma elasticum in a patient with generalized arterial calcification of infancy due to a homozygous missense mutation in the ENPP1 gene. Br J Dermatol 2012;166:1107–11. [PubMed: 22229486]

Li Q, Guo H, Chou DW, Berndt A, Sundberg JP, Uitto J. Mutant Enpp1asj mouse as a model for generalized arterial calcification of infancy. Dis Model Mech 2013;6:1227–35. [PubMed: 23798568]

Li Q, Kingman J, Uitto J. Mineral content of the maternal diet influences ectopic mineralization in offspring of Abcc6 mice. Cell Cycle 2015;14:3184–9. [PubMed: 26199043]

Li Q, Kingman J, Sundberg JP, Levine MA, Uitto J. Dual effects of bisphosphonates on ectopic skin and vascular soft tissue mineralization versus bone microarchitecture in a mouse model of generalized arterial calcification of infancy. J Invest Dermatol 2016;136:275–83. [PubMed: 26763447]

Li Q, Kingman J, van de Wetering K, Tannouri S, Sundberg JP, Uitto J. Abcc6 knockout rat model highlights the role of liver in PPi homeostasis in pseudoxanthoma elasticum. J Invest Dermatol 2017;137:1025–32. [PubMed: 28111129]

Lomashvili KA, Narisawa S, Millan JL, O'Neill WC. Vascular calcification is dependent on plasma levels of pyrophosphate. Kidney Int 2014;85:1351–6. [PubMed: 24717293]

Maddux BA, Chang YN, Accili D, McGuinness OP, Youngren JF, Goldfine ID. Overexpression of the insulin receptor inhibitor PC-1/ENPP1 induces insulin resistance and hyperglycemia. Am J Physiol Endocrinol Metab 2006;290:E746–9. [PubMed: 16278247]

Neldner KH. Pseudoxanthoma elasticum. Clin Dermatol 1988;6:1–159.

Nitschke Y, Baujat G, Botschen U, Wittkampf T, du Moulin M, Stella J, et al. Generalized arterial calcification of infancy and pseudoxanthoma elasticum can be caused by mutations in either ENPP1 or ABCC6. Am J Hum Genet 2012;90:25–39. [PubMed: 22209248]

Orriss IR, Arnett TR, Russell RG. Pyrophosphate: a key inhibitor of mineralisation. Curr Opin Pharmacol 2016;28:57–68. [PubMed: 27061894]

Ringpfeil F, Lebwohl MG, Christiano AM, Uitto J. Pseudoxanthoma elasticum: mutations in the MRP6 gene encoding a transmembrane ATP-binding cassette (ABC) transporter. Proc Natl Acad Sci U S A 2000;97:6001–6. [PubMed: 10811882]

Rutsch F, Ruf N, Vaingankar S, Toliat MR, Suk A, Hohne W, et al. Mutations in ENPP1 are associated with 'idiopathic' infantile arterial calcification. Nature Genet 2003;34:379–81. [PubMed: 12881724]

Scheffer GL, Hu X, Pijnenborg AC, Wijnholds J, Bergen AA, Scheper RJ. MRP6 (ABCC6) detection in normal human tissues and tumors. Lab Invest 2002;82:515–8. [PubMed: 11950908]

Tolouian R, Connery SM, O'Neill WC, Gupta A. Using a filtration technique to isolate platelet free plasma for assaying pyrophosphate. Clin Lab 2012;58:1129–34. [PubMed: 23289181]

Uitto J, Li Q, van de Wetering K, Varadi A, Terry SF. Insights into pathomechanisms and treatment development in heritable ectopic mineralization disorders: Summary of the PXE International Biennial Research Symposium - 2016. J Invest Dermatol 2017;137:790–5. [PubMed: 28340679]

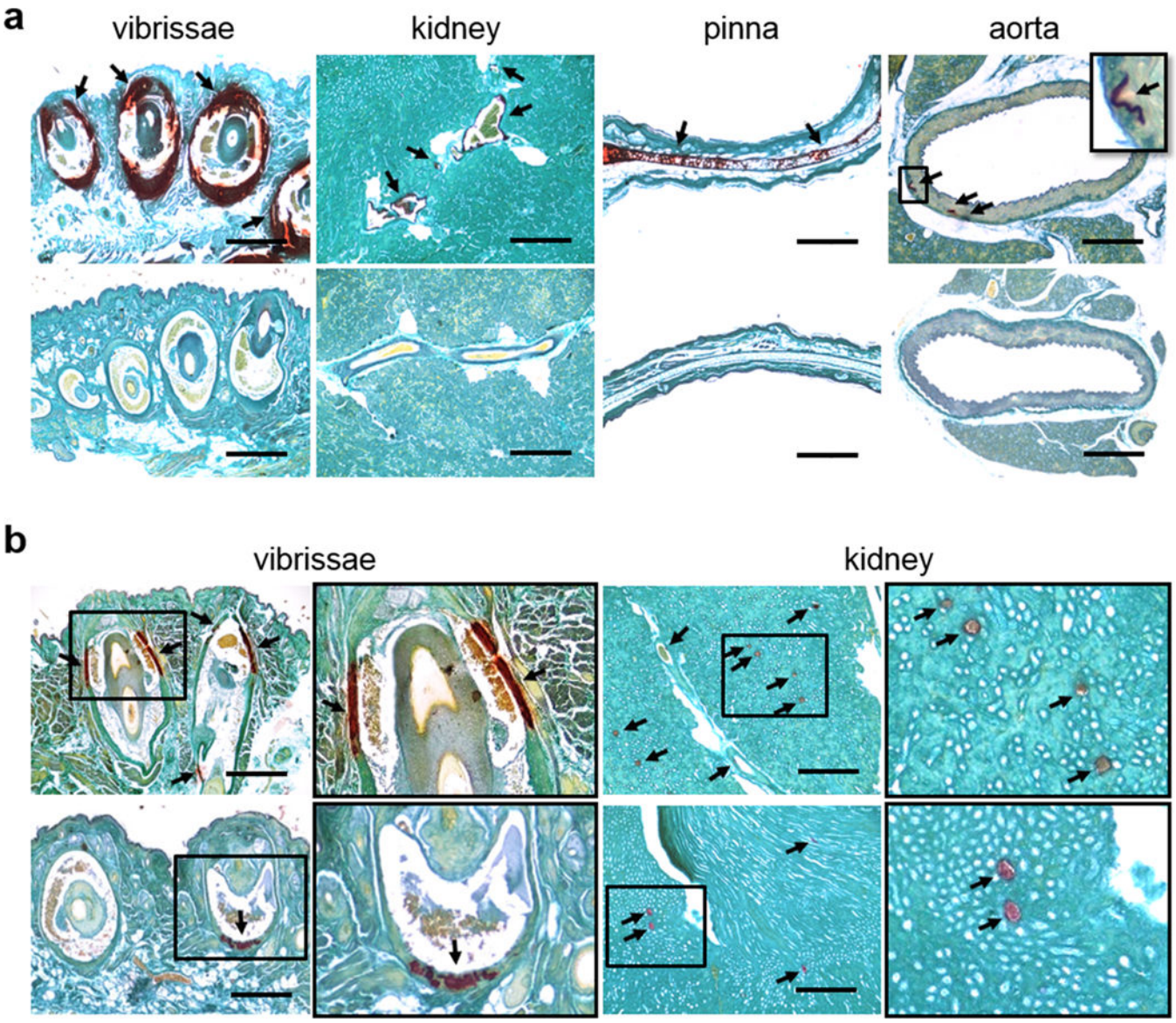

Figure 1. Histopathologic examination demonstrates that overexpression of human ENPP1 completely prevents ectopic connective tissue mineralization in *Enpp1*^{asj} mice but not in *Abcc6*$^{-/-}$ mice.

Tissues were collected in mice on the same diet at 12 weeks of age and analyzed by histopathology with Alizarin red stains. The *Enpp1*^{asj} mice developed ectopic mineralization of the dermal sheath of vibrissae in the muzzle skin, kidney, pinna and aorta (Fig. 1a, upper row). The *Enpp1*^{asj}*;hENPP1*$^{Tg/0}$ mice were entirely negative for mineralization in these tissues (Fig. 1a, lower row). The *Abcc6*$^{-/-}$ mice also developed ectopic mineralization of the dermal sheath of vibrissae in the muzzle skin and in the kidney, although at a lesser extent (Fig. 1b, upper row). The corresponding *Abcc6*$^{-/-}$*;hENPP1*$^{Tg/0}$ mice demonstrated significantly reduced mineralization as compared to *Abcc6*$^{-/-}$*;hENPP1*$^{0/0}$ mice; however, distinct mineralization foci were still evident (Fig. 1b, lower row). Ectopic mineralization is indicated by arrows. Scale bar, 0.4 mm.

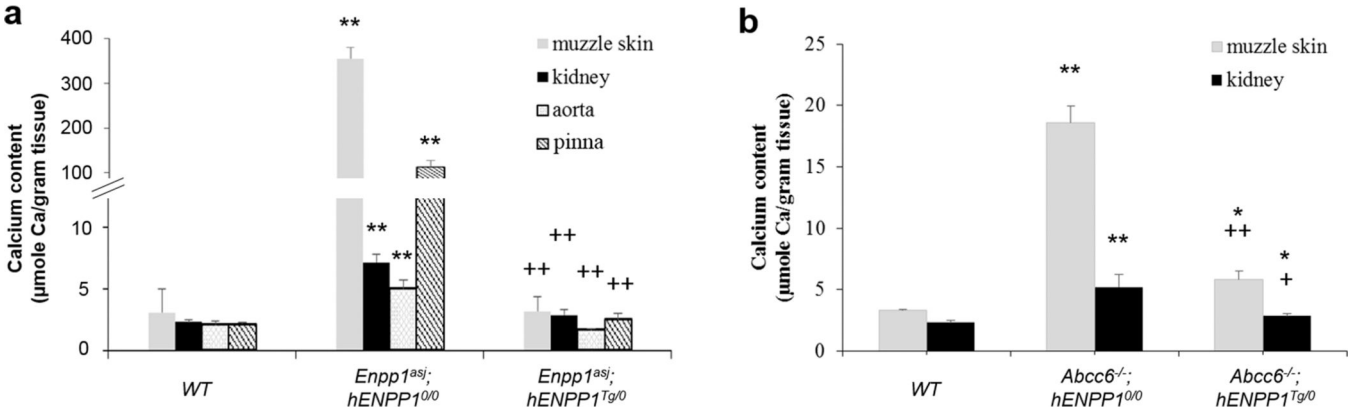

Figure 2. The chemical assay of calcium demonstrates that overexpression of human ENPP1 reduces ectopic connective tissue mineralization in *Enpp1^{asj}* mice and *Abcc6$^{-/-}$* mice.

The calcium content was quantitatively determined in the muzzle skin biopsies containing the dermal sheath of vibrissae, kidney, pinna and aorta in mice on the same diet. Note the significantly elevated calcium content in *Abcc6$^{-/-}$;hENPP1$^{0/0}$* and *Enpp1^{asj};hENPP1$^{0/0}$* mice as compared with the *WT* mice without mineralization. Overexpression of human ENPP1 in *Enpp1^{asj}* mice reduced the calcium content in tissues to that of *WT* mice (a). The calcium content was significantly reduced in *Abcc6$^{-/-}$* mice overexpressing human ENPP1, however, the amount of calcium in the muzzle skin and kidney was still significantly higher than *WT* mice (b). Values were expressed as mean ± SE; n = 11 – 17 mice per group. *WT*, wild type. $^{*}p < 0.05$, $^{**}p < 0.01$, compared with *WT* mice; $^{+}p < 0.05$, $^{++}p < 0.01$, compared with either *Abcc6$^{-/-}$;hENPP1$^{0/0}$* or *Enpp1^{asj};hENPP1$^{0/0}$* mice.

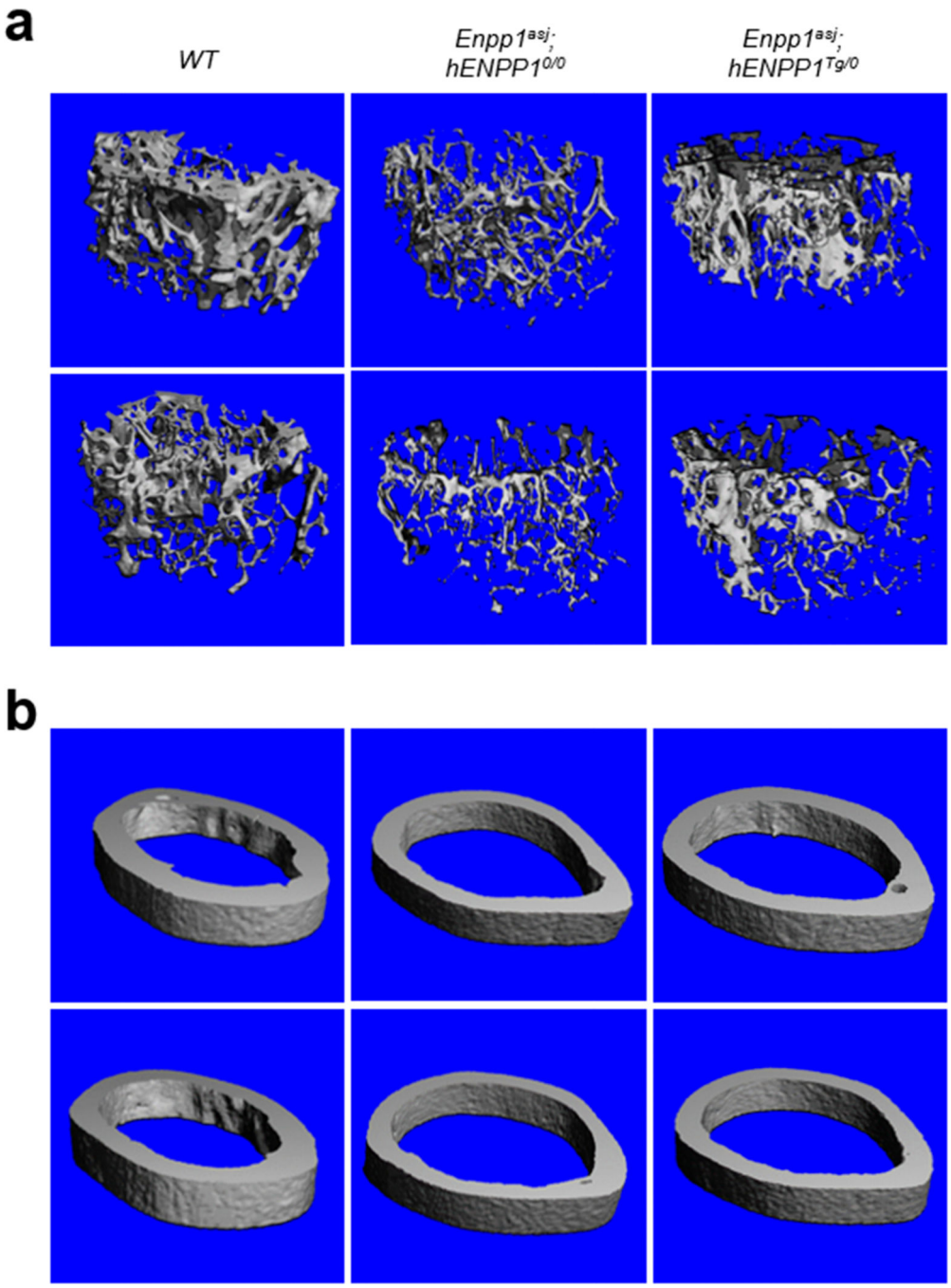

Figure 3. MicroCT analysis reveals changes in bone microarchitecture in *Enpp1^{asj}* mice with overexpression of human ENPP1.

(a) Trabecular bone; (b) cortical bone. The left femurs in the *Enpp1^{asj};hENPP1$^{0/0}$* and *Enpp1^{asj};hENPP1$^{Tg/0}$* mice were compared with *WT* mice on the same diet. Note the distinct differences between male (top row in each panel) and female (bottom row in each panel) mice. Overexpression of human ENPP1 in *Enpp1^{asj}* mice restored the femoral microarchitecture similar to *WT* mice, as quantitatively detailed in Table 3 (n = 4–5 per sex in each group). *WT*, wild type.

Table 1.

Experimental groups of mice by genotype and diet[1)]

Group	Genotype	No. of mice examined (M+F)
A	*WT*	15 (7+8)
B	*hENPP1$^{Tg/0}$*	16 (8+8)
C	*Enpp1^{asj};hENPP1$^{0/0}$*	11 (4+7)
D	*Enpp1^{asj};hENPP1$^{Tg/0}$*	17 (8+9)
E	*Abcc6$^{-/-}$;hENPP1$^{0/0}$*	15 (8+7)
F	*Abcc6$^{-/-}$;hENPP1$^{Tg/0}$*	13 (11+2)

1)All the mice were placed on an “acceleration diet” at 4 weeks of age post-weaning and followed for an additional 8 weeks. Mineralization and blood biochemistry was determined at 12 weeks of age. M, male; F, female.

Table 2.

Blood parameters in different groups of mice

Group	Genotype	Plasma concentration (mean ± S.E.)[1)]				
		Ca^{2+} (mg/dl)	Pi (mg/dl)	Ca/Pi ratio	PPi (μM)	PPi/Pi Ratio, x1,000
A	*WT*	9.45 ± 0.17	8.01 ± 0.46	1.23 ± 0.07	1.12 ± 0.07	2.23 ± 0.17
B	*hENPP1$^{Tg/0}$*	9.34 ± 0.17	7.15 ± 0.22	1.33 ± 0.05	1.88 ± 0.14 *	4.16 ± 0.38 *
C	*Enpp1^{asj};hENPP1$^{0/0}$*	9.27 ± 0.34	7.63 ± 0.44	1.27 ± 0.10	0.01 ± 0.00 *	0.01 ± 0.01 *
D	*Enpp1^{asj};hENPP1$^{Tg/0}$*	9.21 ± 0.32	7.50 ± 0.43	1.29 ± 0.08	0.88 ± 0.06 ≠	1.92 ± 0.18 ≠
E	*Abcc6$^{-/-}$;hENPP1$^{0/0}$*	9.18 ± 0.15	8.36 ± 0.65	1.21 ± 0.12	0.43 ± 0.04 *	0.80 ± 0.07 *
F	*Abcc6$^{-/-}$;hENPP1$^{Tg/0}$*	8.98 ± 0.18	9.11 ± 1.03	1.14 ± 0.12	1.32 ± 0.06 +	2.67 ± 0.35 +

1) Calcium, Pi and PPi levels were measured in plasma samples (n = 11–17 per group).

* $p < 0.01$, compared to wild type (WT) mice in group A

≠ $p < 0.01$, compared to mice in group C

+ $p < 0.01$, compared to mice in group E.

Table 3.

Bone phenotypes by microCT of the right femur of the mice[1)]

Group[2)]	Sex	BMD (mg/cm^3)	BV/TV (%)	Tb.Th (μm)	Tb.N (1/mm)	Tb.Sp (μm)	SMI	Conn.D (TV/mm^3)
Trabecular bone								
A	M	158.9 ± 19.8	9.9 ± 1.8	37.7 ± 9.0	4.4 ± 0.04	222.7 ± 2.7	2.1 ± 0.4	129.5 ± 31.9
A	F	90.2 ± 5.4	4.1 ± 0.6	30.6 ± 2.6	3.6 ± 0.1	277.5 ± 9.2	3.1 ± 0.1	90.8 ± 5.9
C	M	62.8 ± 6.6**	2.5 ± 0.3**	27.8 ± 1.2	3.2 ± 0.2**	310.2 ± 16.5**	3.1 ± 0.2*	40.9 ± 9.9*
C	F	55.9 ± 4.3**	1.8 ± 0.2**	25.8 ± 1.4	3.2 ± 0.1*	308.4 ± 7.7*	3.5 ± 0.1**	16.4 ± 5.0**
D	M	98.9 ± 9.0*,+	4.8 ± 0.6*,+	30.9 ± 0.4+	3.7 ± 0.2*	268.7 ± 16.4*	2.7 ± 0.1	99.1 ± 18.8+
D	F	67.5 ± 4.3*	2.4 ± 0.2*	29.6 ± 0.8+	3.2 ± 0.1*	309.6 ± 8.3*	3.3 ± 0.1*	29.1 ± 7.2**

Group[2)]	Sex	BMD (mg/cm^3)	Ct.Porosity (%)	Ct.pMOI (mm^4)	Ct.Th (μm)
Cortical bone					
A	M	1072.0 ± 6.7	9.4 ± 0.6	0.39 ± 0.04	161.0 ± 6.1
A	F	1111.9 ± 1.0	7.6 ± 0.2	0.31 ± 0.02	161.0 ± 4.1
C	M	1053.3 ± 8.6	12.5 ± 0.3**	0.29 ± 0.01	132.3 ± 3.7**
C	F	1053.5 ± 7.0**	12.5 ± 0.4**	0.27 ± 0.02	132.0 ± 4.7*
D	M	1077.3 ± 11.9	12.1 ± 0.9*	0.39 ± 0.03+	153.4 ± 7.1+
D	F	1069.9 ± 6.0**	11.9 ± 0.3**	0.27 ± 0.01	137.2 ± 3.1**

1)All mice were placed on acceleration diet at 4 weeks of age and maintained for another 8 weeks. The right femurs of the mice were analyzed by microcomputed tomography at 12 weeks of age. Values are expressed as mean ± SE.

2)For a description of different groups, see Table 1.

Abbreviations: M, male; F, female; BMD, bone mineral density; BV/TV, relative bone volume; Tb.Th, trabecular thickness; Tb.N, trabecular number; Tb.Sp, trabecular separation (marrow thickness); SMI, structure model index; Conn.D, connectivity density; Ct.Porosity, cortical porosity; Ct.pMOI, cortical polar moment of inertia; Ct.Th, cortical thickness.

*$p < 0.05$

**$p < 0.01$, compared to WT mice of the same sex on acceleration diet (group A)

$^{+}p < 0.05$, compared to the *asj* mice of the same sex on acceleration diet (group C).